Nano Energy 88 (2021) 106257

Contents lists available at ScienceDirect

Nano Energy

journal homepage: www.elsevier.com/locate/nanoen

Flexible MXene composed triboelectric nanogenerator via facile vacuum-assistant filtration method for self-powered biomechanical sensing☆

Zichao Zhang [a,b,1], Qiuyang Yan [c,d,1], Zhirong Liu [b,d,1], Xinyang Zhao [b], Zhuo Wang [b], Jing Sun [c], Zhong Lin Wang [b,d,*], Ranran Wang [c,e,**], Linlin Li [a,b,d,*]

[a] Center on Nanoenergy Research, School of Physical Science and Technology, Guangxi University, Nanning 530004, PR China
[b] Beijing Institute of Nanoenergy and Nanosystems, Chinese Academy of Sciences, Beijing 101400, PR China
[c] State Key Laboratory of High Performance Ceramics and Superfine Microstructure Shanghai Institute of Ceramics Chinese Academy of Science, Shanghai 200050, PR China
[d] University of Chinese Academy of Sciences, Beijing 100049, PR China
[e] School of Chemistry and Materials Science, Hangzhou Institute for Advanced Study, University of Chinese Academy of Sciences, Hangzhou 310024, PR China

ARTICLE INFO

Keywords:
Triboelectric nanogenerator
MXene
Self-powered
Biomechanical sensing
Wearable sensor

ABSTRACT

With the explosive development of sensing systems in miniaturization, intelligence, multi-function and networking, triboelectric nanogenerator (TENG) with simple structure, low cost and self-powering characters has become an excellent candidate for mechanical sensors. However, it remains a great challenge to obtain a stable interface of electrode and triboelectric layers for timely and long-term triboelectric surface charges transfer. In this study, through a simple vacuum-assistant filtration method, we prepared an integrated MXene-PEDOT:PSS/PTFE (MXene-poly(3,4-ethylenedioxythiophene):Poly (styrenesulfonate)/polytetrafluoroethylene) (MPP) film as the electrode and triboelectric layer of TENG for self-powered sensing. The TENG-based sensor has a high sensitivity especially to tiny forces (>6.05 $V{\cdot}N^{-1}$) with short response (52 ms) and recovery (34 ms) time, as well as an excellent stability (over 6000 cycles). The fabrication method is suitable for most conductive nanomaterials, and the triboelectric layer can be replaced with other commercialized filter films, such as cellulose and mixed fiber resin (MFR). It provides a simple and versatile method for the preparation of stable electrode-triboelectric interface, and has broad prospects in TENG-based wearable sensors.

1. Introduction

In recent years, the demand for real-time health assessment and biomedical monitoring has increased, which poses a high challenge to flexible wearable sensors [1–6]. Different kinds of flexible tactile sensors have been proposed, especially based on the working mechanisms of resistive and capacitive effects [7,8]. Since the first TENG was reported by Wang group in 2012 [9], breakthroughs have been made in the fields of self-powered systems [10–14], self-powered sensors for medical and human bodies [11,15–19], and energy harvesting [4,10,13,20–24]. For wearable tactile sensing, TENGs have the advantages of lightweight, wide material selection, flexible structure design, simple manufacturing process, and high sensitivity [25]. Compared with traditional sensors that require an external power supply to work, TENG-based sensors can directly convert human biomechanical energy into electric signals, thus showing great potentials in the field of wearable and self-powered tactile sensors [1,5,21,26–28].

For wearable tactile sensors, high sensitivity, good flexibility and

☆ Professor Zhong Lin Wang, an author on this paper, is the current Editor-in-Chief of Nano Energy, but he had no involvement in the peer review process used to assess this work submitted to Nano Energy. This paper was assessed and the corresponding peer review managed by Professor Chenguo Hu, an Associate Editor in Nano Energy.

* Corresponding authors at: Beijing Institute of Nanoenergy and Nanosystems, Chinese Academy of Sciences, Beijing 101400, PR China.
** Corresponding author at: State Key Laboratory of High Performance Ceramics and Superfine Microstructure Shanghai Institute of Ceramics Chinese Academy of Science, Shanghai 200050, PR China.
E-mail addresses: zhong.wang@mse.gatech.edu (Z.L. Wang), wangranran@mail.sic.ac.cn (R. Wang), lilinlin@binn.cas.cn (L. Li).
[1] These authors contributed equally to this work.

https://doi.org/10.1016/j.nanoen.2021.106257
Received 1 April 2021; Received in revised form 7 June 2021; Accepted 14 June 2021
Available online 18 June 2021

stability are the worthwhile pursuits. In conventional TENGs, copper or aluminum tapes are stuck onto the triboelectric layer as the electrode layer. It is easy to make, but not suitable for wearable sensing due to their inflexible and uncomfortable nature. In addition, the glue layer of tapes on the electrode or triboelectric layer might hinder the timely and smooth transfer of the generated triboelectric charges from triboelectric layer to electrode, thus inducing recombination of the opposite charges and reducing the output performance. Compared with the bulk conductive layer, electrode layer made from conductive nanomaterials could be fabricated with thinner and more flexible characteristics [29,30]. A common method is to incorporate conductive nanomaterials (such as graphene, carbon nanotubes and silver nanowires) into a non-conductive matrix, which might severely sacrifice the conductivity. Electrodes from organic conductive hydrogel or ionogel have high flexibility and stretchability, but they are often unstable to execute long-term monitoring [31,32]. Other methods to fabricate thin-layer electrodes include magnetron sputtering [33,34] and electron beam evaporation [35,36], both of which could obtain thin and flexible conductive layers. But it is relatively cumbersome and expensive, and the type of material is limited. Thus, it is urgent to obtain flexible electrode layer of TENGs though facile, cost-effective, and generalizable methods.

MXenes are a kind of two-dimensional (2D) materials with composition of transition metal carbides, nitrides or carbonitrides, and their general chemical formula can be represented by $M_{n+1}X_nT_z$, where M refers to transition metals, X refers to C or/and N, n = 1, 2, and 3, Tz refers to surface groups (such as -OH, -O, or -F) [37–40]. With the high conductivity and laminated 2D structure, MXene have been widely used in energy storage, adsorption, sensors and conductive fillers [41,42]. In the recent two years, MXene have been used as a conductive substrate to fabricate TENGs [43–48]. However, in those reports, MXene were only used as conductive additives into the non-conductive substrates, which sacrificed the conductivity.

Herein, using MXene nanosheets as the raw materials, we developed a facile method to fabricate a flexible TENG from integrated film with both electrode and triboelectric layer. Through a one-step vacuum-assistant filtration method, the MXene nanosheets formed an electrode film on the filter film that was directly applied as the triboelectric layer. The integrated film had a tight connection between the electrode and triboelectric layer, allowing timely and smooth transfer of the generated triboelectric charges for a high output. The fabricated TENGs as tactile sensors had a high sensitivity especially for perception of tiny forces (>6.05 $V{\cdot}N^{-1}$), stable cycle performance (over 6000 cycles) and fast response (34–52 ms). Both the solid-liquid contact in the single-electrode mode and the contact-separation mode for self-powered sensing of the human activities showed excellent performance and had the potential for self-powered biomechanical sensing.

2. Experimental section

2.1. Materials

The precursor Ti_3AlC_2 was bought from Forsman Scientific (Beijing) co., Ltd. Hydrochloric acid (HCl) was obtained from Shanghai Titan Scientific co., Ltd. Lithium fluoride (LiF) was purchased from Sinopharm Chemical Reagent co., Ltd. PEDOT:PSS (1000) solution was purchased from Xi'an Polymer Light Technology Corp.

2.2. Fabrication of the MXene

The MXene nanosheets was obtained by selectively etching the A layers in the MAX phase with the help of LiF/HCl. In detail, 6 g LiF was added into 67 mL HCl (6 Mol) to provide F^- and H^+, which can break the chemical bonds between the Ti and Al. Then, 3 g MAX (Ti_3C_2Tx) was added and the mixture was stirred at 60 °C for 48 h. Sediment was collected after washing treatment until the pH of the solution was about 7. After freezing-dried, the obtained sediment was ultrasonicated with a certain volume of water under Ar atmosphere for 2 h to obtain MXene nanosheets with a few lamellar layers. At last, unexfoliated MXene was removed by centrifugation and MXene nanosheets were obtained.

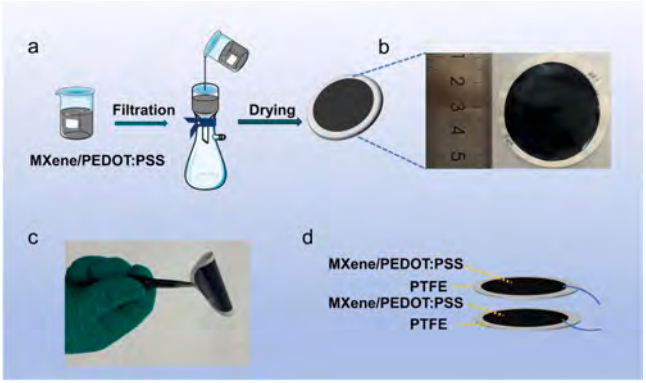

Fig. 1. Illustration of the preparation of MPP film and TENG-based tactile sensor. (a) Schematic illustration of the fabrication of MPP film. (b) Optical image of the prepared MPP film. (c) Photos showing flexibility of the prepared MPP film. (d) Schematic diagram of the MPP film-based TENG sensor.

The MPP film was prepared by a vacuum-assistant filtration. Firstly, PEDOT:PSS was added into MXene solution with a certain ratio (wight: wight = 1:1) and the mixture was stirred for 12 h under a shading condition. Then a certain volume solution was filtrated with a filter film (diameter = 4 cm) composed of PTFE, cellulose or MFR. After being dried in air and dark, the MPP film was obtained. The pure MXene/PTFE films were prepared without the addition of PEDOT:PSS during the vacuum-assistant filtration.

2.3. Characterization and measurement

The morphologies of the obtained films were characterized by a field-emission scanning electron microscope (SU8220, HITACHI, Japan). The surface morphology and roughness of the films was obtained by an atomic force microscope (NTEGRA, NT-MDT, Russia). X-ray diffraction (XRD) characterization was conducted by a high-resolution multifunction X-ray diffractometer (D8 ADVANCE, Bruker, Germany). The fourier transform infrared spectra were recorded with a Fourier transform infrared spectrometer (iN10 iZ10, Thermofisher, the USA). Water contact angles were detected by the XG-CAM Contact Angles Meter (Xuanyichuangxi, China). The 8201 Signal Conditioner was utilized to perform the dynamic pressure measurements (YMC Piozotronics Inc). The electrical performance output and sensing curves were recorded by 6514 SYSTEM Electrometer (Keithley, A Tektronix Company).

3. Results and discussion

The MXene nanosheets were obtained by selectively etching A layers in the Ti_3AlC_2 (MAX phase) with the help of LiF/HCl, which provided F^- and H^+ to break the chemical bonds between the Ti and Al. The resultant MXene nanosheets had a lateral size of 200 nm and a thickness of 3.16 nm (Fig. S1). Fig. 1a schematically illustrates the preparation process of the MXene-based TENG as a mechanical sensor. A continuous, compact, and conductive film could be directly formed on a filter film through vacuum filtration of pure MXene or PEDOT:PSS/MXene hybrids, acting as the electrode layer. The filter film, composed of PTFE, cellulose, or MFR acts not only as a support for the MXene nanosheets to form the electrode layer, but also has a porous surface structure, which directly acts as the triboelectric layer. Thus, the one-step facile vacuum filtration generates a close connection between the electrode layer and the triboelectric layer without any binding agent, which allows for

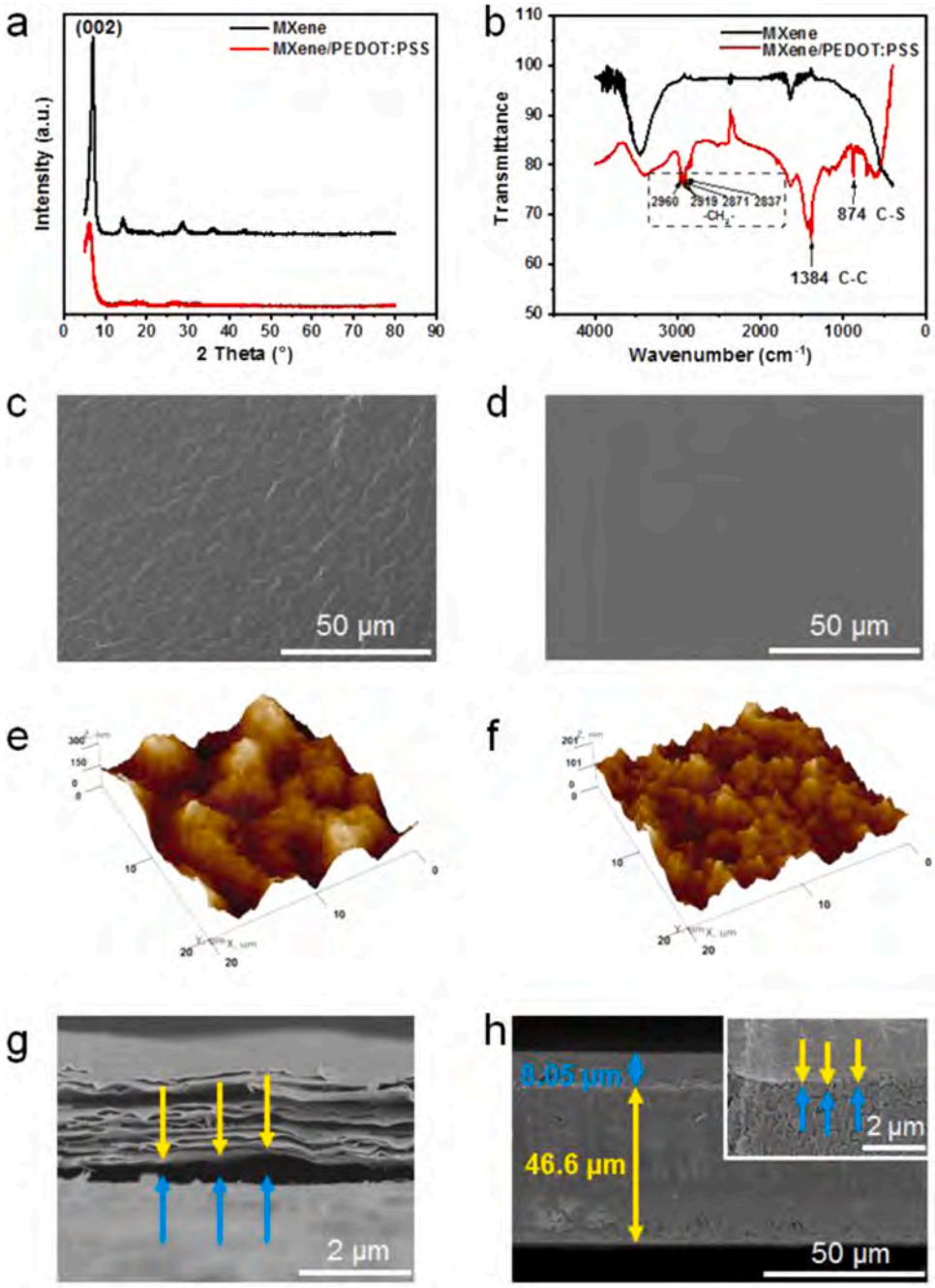

Fig. 2. Characterization of the MXene-PTFE film and MPP film. (a) XRD patterns of pure MXene and MXene/PEDOT:PSS. (b) The Fourier transform infrared absorption spectra of pure MXene and MXene/PEDOT:PSS. Top-view SEM of (c) the MP film without PEDOT:PSS and (d) the MPP film with PEDOT:PSS. AFM image of (e) the MP film without PEDOT:PSS and (f) MXene/PEDOT:PSS film. Cross-section SEM images of (g) MP film without PEDOT:PSS and (h) the MPP film with PEDOT:PSS. The inset is a partial enlarged view.

unobstructed charges transport across the two layers (Fig. 1b). The film prepared by this method is flexible enough for human wearable devices (Fig. 1c). The structure of the MXene-based TENG is shown in Fig. 1d. The bottom MXene film acts as both an electrode and a triboelectric layer, the top PTFE film only serves as a triboelectric layer, and the top MXene film serves as another electrode.

To characterize the output performances of the MXene-based TENG (1 cm × 1 cm), a linear motor was employed to provide periodic contact-separation motions. Under the impulsive force of 1 N and the frequency of 1 Hz, the open circuit voltage (V_{OC}) reached to ~10 V (Fig. S2a). However, the voltage output showed a tendency of attenuation from 10 V to 8 V after 6000 cycles of contact-separation. And the sensor's perception to the external pressures become insensitive. As the pressure increases, the voltage output did not show a regular tendency of increase (Fig. S2b and c). To analyze the reason why the as-prepared MXene-based TENG sensor had a low stability and sensitivity, we observed the morphology of the TENG structure via scanning electron microscopy (SEM). From the cross-sectional view of the integrated MXene-PTFE layer, there was an obvious separation between the electrode and the triboelectric layer (Fig. 2g). Thus, we speculated that the instability output of the TENG sensor was mainly caused by the inadequate contact between the electrode and the triboelectric layer, which affected the transfer of the triboelectric surface charges.

In order to improve the adhesion between the MXene nanosheets-composed electrode layer and the PTFE triboelectric layer, we mixed conductive PEDOT:PSS into the MXene nanosheets with different weight ratio to prepare a MXene-PEDOT:PSS hybrid electrode (MXene-PTFE) via the same process of vacuum filtration. PEDOT:PSS as a kind of conductive polymer has a high electrical conductivity, good mechanical strength and superior stability [49]. By changing the ratio of PEDOT:PSS

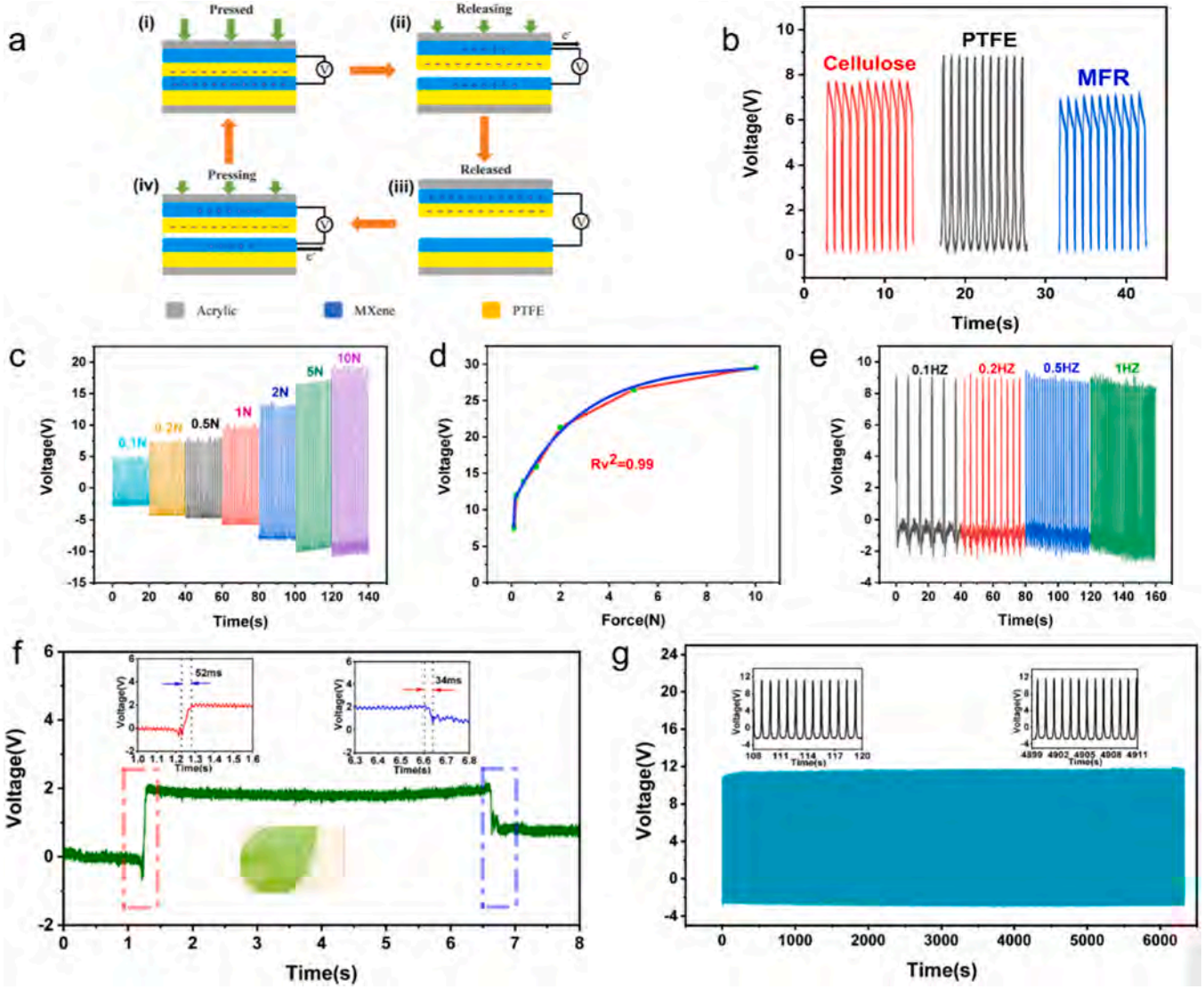

Fig. 3. (a) Working principle of the MXene-based TENG sensor. (b) Voltage output of the TENG based on different triboelectric layers in contact-separation mode. (c) Voltage output of the TENG at the selected forces. (d) Relationship of voltage output of the TENG with force change. (e) Voltage output of the TENG at selected frequencies. (f) Response time and recovery time of the TENG sensor. (g) Voltage output of the TENG under 1 Hz and 1 N impulsive force over 6000 cycles.

incorporated into MXene, the influence of the incorporation of PEDOT:PSS on the performance of TENG based on the MXene composite film was explored. It can be seen from Fig. S3(a–c) that the electrical output of TENG with MXene:(PEDOT:PSS) = 1:1 (w:w) was higher than that of TENG with pure PEDOT:PSS, pure MXene, and MXene:(PEDOT:PSS) = 1:2 and 2:1, so we choose the MXene:(PEDOT:PSS) (1:1) composite film to carry out subsequent experiments. In order to determine the influence of pore size of the filter film on the triboelectric sensors, taking the PTFE filter films as an example, three common PTFE filter films on the market with the pore size of 0.22 μm, 0.45 μm and 1.2 μm were investigated. It can be seen from Fig. S4(a–c) that the electrical performance of the TENG with the film pore size of 0.22 μm was higher than that of the TENG with the film pore size of 0.45 μm. In addition, the output of the TENG made of 1.2 μm filter film was almost zero. It may be due to that the too large pore size of the filter film induced leakage of the MXene (lateral size of ~200 nm) through the film during the suction process, thus making the two electrode layers conductive. Therefore, we choose the MXene composite film with a filter pore size of 0.22 μm to carry out the follow-up experiments.

From the X-ray diffraction (XRD) spectrum of the pure MXene film, there is a main peak at 6.987°, which corresponds to the (002) crystal plane, proving the 2D structure of MXene nanosheets (Fig. 2a). After incorporating PEDOT:PSS, the (002) peak was shifted from 6.987° to 6.291°, confirming the expansion of the interlayer space between the MXene nanosheets, which corresponds to 13 nm and 14 nm, respectively [50]. From the Fourier transform infrared spectra of the pure MXene and MXene-PTFE films (Fig. 2b), several new characteristic peaks appeared after the addition of PEDOT:PSS. In detail, the new peaks appearing at 2919 cm^{-1} and 2871 cm^{-1} corresponds to the stretching vibration peak of -CH_2-, while peak at 1384 cm^{-1} is related to the stretching vibration peak of C-C. And the peak at 874 cm^{-1} is related to C-S band. All these new peaks reveal the existence of PEDOT:PSS in the hybrid film [51]. Compared with the pure MXene film, the surface wrinkles (4–6 μm) of MXene-PTFE film decreased while the number of particles (< 1 μm) increased (Figs. 2c, d and S6). The atomic force microscopy (AFM) images and statistic parameters (Fig. 2e and f) shows that the roughness of the MXene-PTFE film was significantly reduced from 65.06 nm to 24.626 nm of pure MXene film. These results indicated that PEDOT:PSS was successfully incorporated into MXene. The pure MXene film showed a clearly layered and stacked structure with many intervals, whereas the MXene-PTFE film was compact without an obvious layered structure (Fig. 2g). From the cross-sectional SEM image

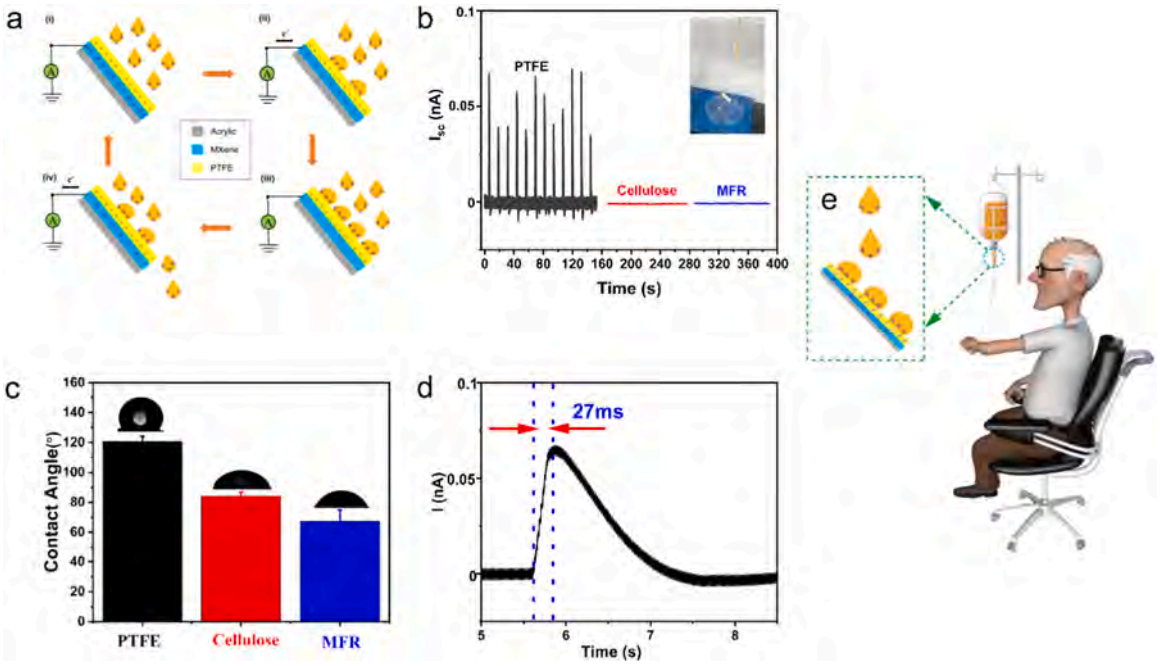

Fig. 4. (a) Schematic diagram of the principle of water droplets falling on the single-electrode mode TENG. (b) Current output of the single-electrode mode TENGs with MFR, PTFE and cellulose as the triboelectric layers. The inset is the installation diagram during measurement. (c) Contact angles of the three different triboelectric layers in contact with the water droplets. (d) Current curve of the TENG pressed by a small water droplet. (e) The application of the single-electrode mode TENG in biomedicine.

of the integrated electrode/ triboelectric layer from MXene-PTFE and PTFE film (Fig. 2h), the thickness of the MXene-PTFE electrode layer was about 8.05 μm, and the thickness of the PTFE triboelectric layer was about 46.6 μm. It was found that the MXene-PTFE layer and PTFE layer were tightly adhered. We deduced that the incorporated PEDOT:PSS could not only tightly connect the MXene nanosheets together in the electrode film, but also be embedded in the pores on the surface of the PTFE film facing the electrode to improve the adhesion of the electrode layer and the triboelectric layer (arrow in Fig. 2h). These results indicated that the integration of PEDOT:PSS with MXene nanosheets for the electrode film could increase the adhesion of the electrode layer with the triboelectric layer.

The working principle of the TENG is based on electrostatic induction and triboelectric effect. Under an external pressure, the bottom MXene-PTFE electrode and the top PTFE layer are in contact, and equal opposite charges are generated at the interface of the two films due to the difference in the triboelectricity of the films (Fig. 3a). In detail, positive charges are generated at the MXene-PTFE electrode and negative charges on the PTFE triboelectric layer. With release of the external pressure, the MXene-PTFE electrode and the triboelectric layer gradually move away. In order to balance the positive charges on the bottom electrode, free electrons move from the top electrode to the bottom electrode, thus generating an instantaneous current. When the external force is re-applied on the TENG and the two films come into contact again, the original electrostatic balance is broken, and electrons flow from the bottom electrode back to the top electrode, generating an opposite output signal. With the regular contact-separation between the films, a stable alternating current would be generated. For the triboelectric layer, the PTFE film could also be replaced with other commercial filter films, such as cellulose and MFR. Under the same magnitude of force and frequency (0.7 N; 1 Hz), the maximum voltage output of the MXene-PTFE TENG with PTFE, cellulose and MFR as the triboelectric layer were 8.8 V, 7.8 V and 7 V, respectively (Fig. 3b). It was caused by the different triboelectric properties of these triboelectric layers. In the following experiment, PTFE layers were used in the TENG sensors because of their high voltage output, high hydrophobicity, and stability. As the external force gradually increased from 0.1 to 10 N, the voltage output of the MPP TENG were also increased from 7.52 V to 29.56 V (Fig. 3c). In addition, the relationship between the voltage and the pressure acting on the sensor had an exponential function relationship by fitting the experimental data:

$$y = y_0 + A_1*(1 - \exp(-x/t_1)) + A_2*(1 - \exp(-x/t_2))$$

In this equation, $y_0 = 9.93$, $A_1 = 16.90$, $t_1 = 2.17$, $A_2 = 1.14 \times 10^{15}$, and $t_2 = 4.00 \times 10^{15}$. Effective isotropic sensitivity is an important index used to evaluate the accuracy of the sensor, which refers to the magnitude of the electrical response under pressure stimulation. It could be calculated based on the equation:

$$s = \frac{dv}{dF}$$

Where S is the sensitivity, V is the quantitative output signal and F is the applied external pressure. According to the relationship curve between force and voltage (Fig. 3d), the sensitivity of the sensor gradually increased as the force decreased, and its sensitivity was higher than 6.05 V N^{-1} when the force was low than 0.5 N. Generally speaking, the force generated by human activity is low, which requires the sensor to have a low detection limit and a high sensitivity, especially in the range of low forces. As shown in Fig. S16, compared with the other reported TENG-based sensors, the prepared MPP-TENG showed a high sensitivity (Voltage/Force) [52–58]. This was mainly because the integrated MPP film prepared by the vacuum-assistant filtration method had a tight connection between the electrode and the triboelectric layer, allowing timely transfer of the generated triboelectric charges. Based on the pressure sensitivity, the MPP TENG sensor can meet the requirement of self-powered human biomechanical sensing for personal healthcare monitoring. Fig. 3e shows the output voltage of the TENG under different frequencies in the range of 0.1–1 Hz, matching the frequencies of normal human movement. The peak value and shape of the voltage signal at the selected frequency were highly consistent, which proved that the TENG sensor can meet the requirements of reciprocating multi-frequency motion sensing. Response time is also an important

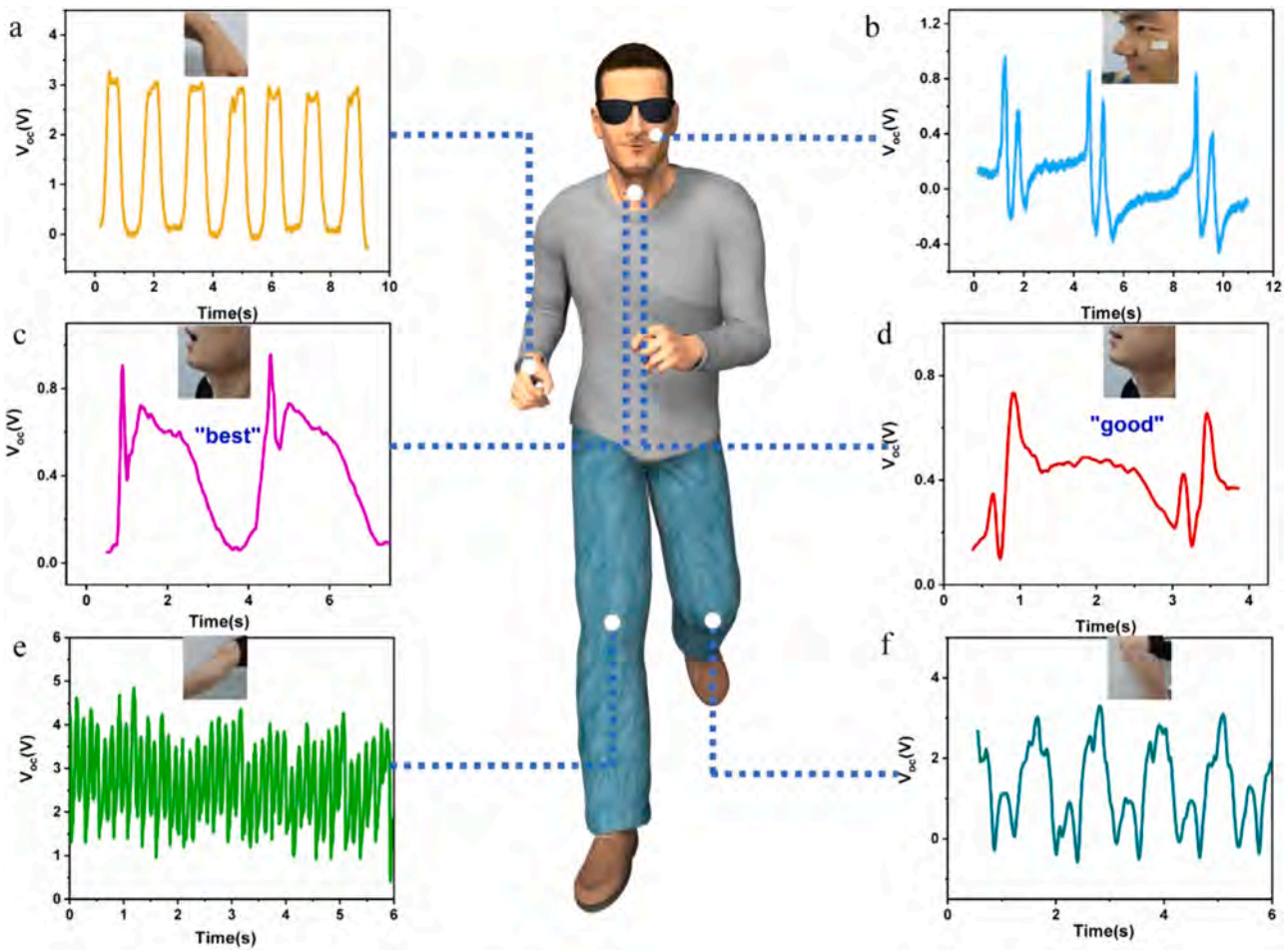

Fig. 5. Application of the TENG sensors for monitoring various physiological movements of the human body. (a) Wrist exercising. (b) Facial expression changing. (c–d) Voltage output in response to these pronunciations of "good" and "best". (e–f) Changes of voltage signal in different exercise modes.

basis for measuring the performance of a sensor. To detect the sensitivity and response time of the TENG sensor, a green leaf with a weight of 0.1926 g (corresponding to a tiny force of 1.93×10^{-3} N) was fallen on the TENG sensor. The TENG sensor could immediately respond to the action and the response time was as short as 52 ms. When the green leaf was removed, the recovery time of the sensor was only 34 ms (Fig. 3f). These results proved the sensor had a low detection limit, high sensitivity and short response time. The cycle stability test of the TENG sensor is shown in Fig. 3g. The TENG sensor maintained a stable electrical output after 6000 contact-separation cycles. It proved that the TENG had a good sensing stability to realize a long-term self-powered sensing.

The TENG sensor can also work in a single-electrode-mode for solid-liquid triboelectric sensing. The structure of the single electrode mode TENG was shown in Fig. 4a and Video S1. The TENG was fixed on the petri dish at a fixed angle of 60° with an acrylic plate. Deionized water was dropped onto the TENG sensor dropwise, and the dropping rate was controlled by a peristaltic pump. In the initial stage, the water droplets are positively charged due to the environmental factors [59]. In the device charge saturation state, when the droplet comes into contact with the PTFE triboelectric layer, electrons are transferred from the ground to the MXene-PTFE electrode, generating a transient positive current driven by the potential difference. When the droplet leaves the surface of the single-electrode-mode triboelectric layer, a negative potential is generated between the MXene-PTFE electrode and the ground, driving the electrons to flow from the electrode to the ground and producing an instantaneous negative current. Under the continuous drop of liquid droplets, a stable electrical signal output can be generated (Fig. 4a). To optimize the performance, we detected the output of the single-electrode-mode TENG with MFR, PTFE and cellulose as the triboelectric layers, respectively (Fig. 4b). It can be clearly seen that only the TENG using PTFE film as the triboelectric layer had a current output (~0.03–0.07 nA), while MXene-based TENG using MFR film or cellulose film as the triboelectric layer both had no obvious current output. This might be due to the hydrophilicity of the MFR film (water contact angle (CA = 67.2°) and the cellulose film (CA = 84.2°). The water droplets could infiltrate the surface of the hydrophilic film that would suppress the generation of triboelectric charges. In contrast, the PTFE film was hydrophobic (CA = 120.6°), which ensured the smooth flow of the water droplets without affecting the properties of the triboelectric and the electrode layer, thereby generating a continuous pulse current output (Fig. 4c). As shown in Fig. 4d, the responsive time of the TENG sensor to the droplets falling was 27 ms. It showed that the single-electrode-mode TENG with a solid-liquid friction had the possibility to sense the actions at those solid-liquid contact interfaces. It can be applied as a droplet sensor in biomedical field (Fig. 4e). The sensor can accurately monitor infusion and clinical drainage operations in real-time, reducing the work intensity of medical staff, and providing timely and effective care for patients.

Supplementary material related to this article can be found online at doi:10.1016/j.nanoen.2021.106257.

With the good pressure response and high sensitivity, the designed TENG sensor was used to monitor different physiological movements of human body. Fluorinated ethylene propylene (FEP) film was used to encapsulate the MPP TENG to ensure that the wearable TENG could be attached at any place of the body for sensing flexibly. The wrist is one part of human body with frequent motions. When the TENG sensor was

attached on the wrist of a volunteer, the TENG sensor generated voltage pulses of 2.9 V with the regular movement of the wrist (Fig. 5a). When the sensor was lightly attached to face, the subtle change of facial expressions induced voltage pulses with 1.1 V (Fig. 5b). Thus, the facial expressions could be monitored by the TENG sensor. The sensor also had a good voice perception. It was found that the voltage changes presented by the TENG sensor to different sounds were unique and repeatable. Here we took "good" and "best" as examples. It can be clearly found that the voltage output of the TENG had different modes in the process of pronouncing of "good" and "best" (Fig. 5c–d). In order to prove that the signal generation was regular, we read these two words twice and the signals were stable and consistent. Based on the voltage signals of the TENG sensor attached to the knee, it could distinguish the different states of human exercise through the amplitude and frequency of the signal changes. Compared with the high-frequency running, normal walking produced a lower voltage output and frequency (Fig. 5e and f). The above applications for human motion monitoring demonstrated the excellent performance of the prepared TENG-based sensor for tactile sensing in wearable electronics, and may provide an alternative way of communication for deaf-mutes.

4. Conclusions

In summary, through a facile vacuum-assistant filtration process, an integrated MPP film with both MXene electrode and triboelectric layer could be directly prepared. The two layers were tightly connected, allowing free transfer of the generated triboelectric charges for a high TENG performance. The MPP-based TENG sensor had a high sensitivity to tiny forces with a sensitivity $>6.05\ V{\cdot}N^{-1}$, fast response (52 ms) and recovery (34 ms) time and excellent durability (over 6000 cycles). It can be used as a self-powered flexible sensor with a good signal response both in the single-electrode mode for solid-liquid contact and the contact-separation mode for human body sensing, such as human facial expressions and voices. These results proved the great potential of this TENG-based sensor prepared in biomedicine and personal wearable medical devices.

CRediT authorship contribution statement

Zichao Zhang: Conceptualization, Methodology, Visualization, Data curation, Writing - original draft. **Qiuyang Yan:** Methodology, Validation, Resources, Writing - review & editing. **Zhirong Liu:** Methodology, Data curation, Writing - review & editing. **Xinyang Zhao**: Methodology, Visualization. **Zhuo Wang**: Methodology, Writing - review & editing. **Jing Sun**: Resources, Methodology. **Zhong Lin Wang**: Conceptualization, Supervision. **Ranran Wang:** Resources, Conceptualization, Methodology, Supervision. **Linlin Li**: Supervision, Conceptualization, Supervision, Writing - review & editing.

Declaration of Competing Interest

The authors declare that they have no known competing financial interests or personal relationships that could have appeared to influence the work reported in this paper.

Acknowledgements

The work was supported by the National Key R&D project from Minister of Science and Technology, China (2016YFA0202703), the National Natural Science Foundation of China (No. 82072065, 81471784), Austrian-Chinese Cooperative R&D Projects (GJHZ2046), Youth Innovation Promotion Association CAS (Y201841), the National Youth Talent Support Program, and China Postdoctoral Science Foundation (No. BX2021299).

Appendix A. Supporting Information

Supplementary data associated with this article can be found in the online version at doi:10.1016/j.nanoen.2021.106257.

References

[1] F.R. Fan, W. Tang, Z.L. Wang, Flexible nanogenerators for energy harvesting and self-powered electronics, Adv. Mater. 28 (2016) 4283–4305.
[2] X. Pu, L. Li, H. Song, C. Du, Z. Zhao, C. Jiang, G. Cao, W. Hu, Z.L. Wang, A self-charging power unit by integration of a textile triboelectric nanogenerator and a flexible lithium-ion battery for wearable electronics, Adv. Mater. 27 (2015) 2472–2478.
[3] X. Pu, M. Liu, X. Chen, J. Sun, C. Du, Y. Zhang, J. Zhai, W. Hu, Z.L. Wang, Ultrastretchable, transparent triboelectric nanogenerator as electronic skin for biomechanical energy harvesting and tactile sensing, Sci. Adv. 3 (2017), e1700015.
[4] Y. Zi, H. Guo, Z. Wen, M.H. Yeh, C. Hu, Z.L. Wang, Harvesting low-frequency (<5 Hz) irregular mechanical energy: a possible killer application of triboelectric nanogenerator, ACS Nano 10 (2016) 4797–4805.
[5] G. Zhu, Y.S. Zhou, P. Bai, X.S. Meng, Q. Jing, J. Chen, Z.L. Wang, A shape-adaptive thin-film-based approach for 50% high-efficiency energy generation through micro-grating sliding electrification, Adv. Mater. 26 (2014) 3788–3796.
[6] G. Shan, X. Li, W. Huang, AI-enabled wearable and flexible electronics for assessing full personal exposures, Innovation 1 (2020), 100031.
[7] J. Chen, Z.L. Wang, Reviving vibration energy harvesting and self-powered sensing by a triboelectric nanogenerator, Joule 1 (2017) 480–521.
[8] Y. Zhang, M. Peng, Y. Liu, T. Zhang, Q. Zhu, H. Lei, S. Liu, Y. Tao, L. Li, Z. Wen, X. Sun, Flexible self-powered real-time ultraviolet photodetector by coupling triboelectric and photoelectric effects, ACS Appl. Mater. Interfaces 12 (2020) 19384–19392.
[9] Z.L. Wang, Triboelectric nanogenerators as new energy technology for self-powered systems and as active mechanical and chemical sensors, ACS Nano 7 (2013) 9533–9557.
[10] X. Cao, Y. Jie, N. Wang, Z.L. Wang, Triboelectric nanogenerators driven self-powered electrochemical processes for energy and environmental science, Adv. Energy Mater. 6 (2016), 1600665.
[11] H.T. Chen, Y. Song, H. Guo, L.M. Miao, X.X. Chen, Z.M. Su, H.X. Zhang, Hybrid porous micro structured finger skin inspired self-powered electronic skin system for pressure sensing and sliding detection, Nano Energy 51 (2018) 496–503.
[12] J. Nie, Z. Ren, J. Shao, C. Deng, L. Xu, X. Chen, M. Li, Z.L. Wang, Self-powered microfluidic transport system based on triboelectric nanogenerator and electrowetting technique, ACS Nano 12 (2018) 1491–1499.
[13] J. Chen, J. Yang, Z. Li, X. Fan, Y. Zi, Q. Jing, H. Guo, Z. Wen, K.C. Pradel, S. Niu, Z. L. Wang, Networks of triboelectric nanogenerators for harvesting water wave energy: a potential approach toward blue energy, ACS Nano 9 (2015) 3324–3331.
[14] Z. Liu, J. Nie, B. Miao, J. Li, Y. Cui, S. Wang, X. Zhang, G. Zhao, Y. Deng, Y. Wu, Z. Li, L. Li, Z.L. Wang, Self-powered intracellular drug delivery by a biomechanical energy-driven triboelectric nanogenerator, Adv. Mater. 31 (2019), e1807795.
[15] W. Xu, L.B. Huang, M.C. Wong, L. Chen, J. Hao, Self-powered sensors: environmentally friendly hydrogel-based triboelectric nanogenerators for versatile energy harvesting and self-powered sensors, Adv. Energy Mater. 7 (2017), 1601529.
[16] Y.-T. Jao, P.-K. Yang, C.-M. Chiu, Y.-J. Lin, S.-W. Chen, D. Choi, Z.-H. Lin, A textile-based triboelectric nanogenerator with humidity-resistant output characteristic and its applications in self-powered healthcare sensors, Nano Energy 50 (2018) 513–520.
[17] X. Ding, H. Cao, X. Zhang, M. Li, Y. Liu, Large scale triboelectric nanogenerator and self-powered flexible sensor for human sleep monitoring, Sensors 18 (2018) 1713.
[18] Z.X. Liu, Z.Z. Zhao, X.W. Zeng, X.L. Fu, Y. Hu, Expandable microsphere-based triboelectric nanogenerators as ultrasensitive pressure sensors for respiratory and pulse monitoring, Nano Energy 59 (2019) 295–301.
[19] M. Zhu, Q. Shi, T. He, Z. Yi, Y. Ma, B. Yang, T. Chen, C. Lee, Self-powered and self-functional cotton sock using piezoelectric and triboelectric hybrid mechanism for healthcare and sports monitoring, ACS Nano 13 (2019) 1940–1952.
[20] J. Wang, C. Wu, Y. Dai, Z. Zhao, A. Wang, T. Zhang, Z.L. Wang, Achieving ultrahigh triboelectric charge density for efficient energy harvesting, Nat. Commun. 8 (2017) 88.
[21] X.F. Wang, S.M. Niu, Y.J. Yin, F. Yi, Z. You, Z.L. Wang, Triboelectric nanogenerator based on fully enclosed rolling spherical structure for harvesting low-frequency water wave energy, Adv. Energy Mater. 5 (2015), 1501467.
[22] C.S. Wu, A.C. Wang, W.B. Ding, H.Y. Guo, Z.L. Wang, Triboelectric nanogenerator: a foundation of the energy for the new era, Adv. Energy Mater. 9 (2019), 1802906.
[23] J.W. Zhong, Q.Z. Zhong, F.R. Fan, Y. Zhang, S.H. Wang, B. Hu, Z.L. Wang, J. Zhou, Finger typing driven triboelectric nanogenerator and its use for instantaneously lighting up LEDs, Nano Energy 2 (2013) 491–497.
[24] T. He, Q. Shi, H. Wang, F. Wen, T. Chen, J. Ouyang, C. Lee, Beyond energy harvesting - multi-functional triboelectric nanosensors on a textile, Nano Energy 57 (2019) 338–352.
[25] S. Wang, M. He, B. Weng, L. Gan, Y. Zhao, N. Li, Y. Xie, Stretchable and wearable triboelectric nanogenerator based on kinesio tape for self-powered human motion sensing, Nanomaterials 8 (2018) 657.
[26] Y.C. Lai, J. Deng, S.L. Zhang, S. Niu, H. Guo, Z.L. Wang, Single-thread-based wearable and highly stretchable triboelectric nanogenerators and their

applications in cloth-based self-powered human-interactive and biomedical sensing, Adv. Funct. Mater. 27 (2017), 1604462.
[27] Z. Lin, J. Chen, X. Li, Z. Zhou, K. Meng, W. Wei, J. Yang, Z.L. Wang, Triboelectric nanogenerator enabled body sensor network for self-powered human heart-rate monitoring, ACS Nano 11 (2017) 8830–8837.
[28] C.F. Guo, L. Ding, Integration of soft electronics and biotissues, Innovation 2 (2021), 100074.
[29] Y. Jiang, K. Dong, X. Li, J. An, D.Q. Wu, X. Peng, J. Yi, C. Ning, R.W. Cheng, P. T. Yu, Z.L. Wang, Stretchable, washable, and ultrathin triboelectric nanogenerators as skin-like highly sensitive self-powered haptic sensors, Adv. Funct. Mater. 31 (2021), 2005584.
[30] X. Peng, K. Dong, C.Y. Ye, Y. Jiang, S.Y. Zhai, R.W. Cheng, D. Liu, X.P. Gao, J. Wang, Z.L. Wang, A breathable, biodegradable, antibacterial, and self-powered electronic skin based on all-nanofiber triboelectric nanogenerators, Sci. Adv. 6 (2020), eaba9624.
[31] Y. Liu, J. Liu, S. Chen, T. Lei, Y. Kim, S. Niu, H. Wang, X. Wang, A.M. Foudeh, J. B. Tok, Z. Bao, Soft and elastic hydrogel-based microelectronics for localized low-voltage neuromodulation, Nat. Biomed. Eng. 3 (2019) 58–68.
[32] G.R. Zhao, Y.W. Zhang, N. Shi, Z.R. Liu, X.D. Zhang, M.Q. Wu, C.F. Pan, H.L. Liu, L. L. Li, Z.L. Wang, Transparent and stretchable triboelectric nanogenerator for self-powered tactile sensing, Nano Energy 59 (2019) 302–310.
[33] Q.Z. Guo, L.C. Yang, R.C. Wang, C.P. Liu, Tunable work function of $Mg_xZn_{1-x}O$ as a viable friction material for a triboelectric nanogenerator, ACS Appl. Mater. Interfaces 11 (2019) 1420–1425.
[34] J. Zhu, Y. Zhu, W. Song, H. Wang, M. Gao, M. Cho, I. Park, Zinc oxide-enhanced piezoelectret polypropylene microfiber for mechanical energy harvesting, ACS Appl. Mater. Interfaces 10 (2018) 19940–19947.
[35] B.D. Chen, D. Liu, T. Jiang, W. Tang, Z.L. Wang, A triboelectric closed-loop sensing system for authenticity identification of paper-based artworks, Adv. Mater. Technol. 5 (2020), 2000194.
[36] T. Kim, S. Jeon, S. Lone, S.J. Doh, D.-M. Shin, H.K. Kim, Y.-H. Hwang, S.W. Hong, Versatile nanodot-patterned Gore-Tex fabric for multiple energy harvesting in wearable and aerodynamic nanogenerators, Nano Energy 54 (2018) 209–217.
[37] M. Ghidiu, M.R. Lukatskaya, M.Q. Zhao, Y. Gogotsi, M.W. Barsoum, Conductive two-dimensional titanium carbide 'clay' with high volumetric capacitance, Nature 516 (2014) 78–81.
[38] M.R. Lukatskaya, O. Mashtalir, C.E. Ren, Y. Dall'Agnese, P. Rozier, P.L. Taberna, M. Naguib, P. Simon, M.W. Barsoum, Y. Gogotsi, Cation intercalation and high volumetric capacitance of two-dimensional titanium carbide, Science 341 (2013) 1502–1505.
[39] M. Naguib, O. Mashtalir, J. Carle, V. Presser, J. Lu, L. Hultman, Y. Gogotsi, M. W. Barsoum, Two-dimensional transition metal carbides, ACS Nano 6 (2012) 1322–1331.
[40] M. Naguib, V.N. Mochalin, M.W. Barsoum, Y. Gogotsi, 25th Anniversary Article: MXenes: a new family of two-dimensional materials, Adv. Mater. 26 (2014) 992–1005.
[41] Y.N. Yang, Z.R. Cao, P. He, L.J. Shi, G.Q. Ding, R.R. Wang, J. Sun, Ti_3C_2Tx MXene-graphene composite films for wearable strain sensors featured with high sensitivity and large range of linear response, Nano Energy 66 (2019), 104134.
[42] Y.N. Yang, L.J. Shi, Z.R. Cao, R.R. Wang, J. Sun, Strain sensors with a high sensitivity and a wide sensing range based on a Ti_3C_2Tx (MXene) nanoparticle-nanosheet hybrid network, Adv. Funct. Mater. 29 (2019), 1807882.
[43] T. Bhatta, P. Maharjan, H. Cho, C. Park, S.H. Yoon, S. Sharma, M. Salauddin, M. T. Rahman, S.M.S. Rana, J.Y. Park, High-performance triboelectric nanogenerator based on MXene functionalized polyvinylidene fluoride composite nanofibers, Nano Energy 81 (2021), 105670.
[44] C.M. Jiang, C. Wu, X.J. Li, Y. Yao, L.Y. Lan, F.N. Zhao, Z.Z. Ye, Y.B. Ying, J.F. Ping, All-electrospun flexible triboelectric nanogenerator based on metallic MXene nanosheets, Nano Energy 59 (2019) 268–276.
[45] Y.-W. Cai, X.-N. Zhang, G.-G. Wang, G.-Z. Li, D.-Q. Zhao, N. Sun, F. Li, H.-Y. Zhang, J.-C. Han, Y. Yang, A flexible ultra-sensitive triboelectric tactile sensor of wrinkled PDMS/MXene composite films for E-skin, Nano Energy 81 (2021), 105663.
[46] M. Salauddin, S.M.S. Rana, M. Sharifuzzaman, M.T. Rahman, C. Park, H. Cho, P. Maharjan, T. Bhatta, J.Y. Park, A novel MXene/ecoflex nanocomposite-coated fabric as a highly negative and stable friction layer for high-output triboelectric nanogenerators, Adv. Energy Mater. 11 (2020), 2002832.
[47] W. He, M. Sohn, R. Ma, D.J. Kang, Flexible single-electrode triboelectric nanogenerators with MXene/PDMS composite film for biomechanical motion sensors, Nano Energy 78 (2020), 105383.
[48] W.-T. Cao, H. Ouyang, W. Xin, S. Chao, C. Ma, Z. Li, F. Chen, M.-G. Ma, A stretchable highoutput triboelectric nanogenerator improved by MXene liquid electrode with high electronegativity, Adv. Funct. Mater. 30 (2020), 2004181.
[49] W. Guo, X. Zhang, X. Yu, S. Wang, J. Qiu, W. Tang, L. Li, H. Liu, Z.L. Wang, Self-powered electrical stimulation for enhancing neural differentiation of mesenchymal stem cells on graphene–poly(3,4-ethylenedioxythiophene) hybrid microfibers, ACS Nano 10 (2016) 5086–5095.
[50] M. Naguib, M. Kurtoglu, V. Presser, J. Lu, J. Niu, M. Heon, L. Hultman, Y. Gogotsi, M.W. Barsoum, Two-dimensional nanocrystals produced by exfoliation of Ti_3AlC_2, Adv. Mater. 23 (2011) 4248–4253.
[51] L. Wang, L.X. Chen, P. Song, C.B. Liang, Y.J. Lu, H. Qiu, Y.L. Zhang, J. Kong, J. W. Gu, Fabrication on the annealed Ti_3C_2Tx MXene/epoxy nanocomposites for electromagnetic interference shielding application, Compos Part B Eng. 171 (2019) 111–118.
[52] G. Zhao, Y. Zhang, N. Shi, Z. Liu, X. Zhang, M. Wu, C. Pan, H. Liu, L. Li, Z.L. Wang, Transparent and stretchable triboelectric nanogenerator for self-powered tactile sensing, Nano Energy 59 (2019) 302–310.
[53] G. Zhao, X. Zhang, X. Cui, S. Wang, Z. Liu, L. Deng, A. Qi, X. Qiao, L. Li, C. Pan, Y. Zhang, L. Li, Piezoelectric polyacrylonitrile nanofiber film-based dual-function self-powered flexible sensor, ACS Appl. Mater. Interfaces 10 (2018) 15855–15863.
[54] P. Wang, R. Liu, W. Ding, P. Zhang, L. Pan, G. Dai, H. Zou, K. Dong, C. Xu, Z. L. Wang, Complementary Electromagnetic-triboelectric active sensor for detecting multiple mechanical triggering, Adv. Funct. Mater. 28 (2018), 1705808.
[55] H. Wu, Q. Shi, F. Wang, A.V.-Y. Thean, C. Lee, Self-powered cursor using a triboelectric mechanism, Small Methods 2 (2018), 1800078.
[56] Z. Lin, Q. He, Y. Xiao, T. Zhu, J. Yang, C. Sun, Z. Zhou, H. Zhang, Z. Shen, J. Yang, Z.L. Wang, Flexible timbo-like triboelectric nanogenerator as self-powered force and bend sensor for wireless and distributed landslide monitoring, Adv. Mater. Technol. 3 (2018), 1800144.
[57] C. Lu, J. Chen, T. Jiang, G. Gu, W. Tang, Z.L. Wang, A stretchable, flexible triboelectric nanogenerator for self-powered real-time motion monitoring, Adv. Mater. Technol. 3 (2018), 1800021.
[58] M. Li, Y. Jie, L.-H. Shao, Y. Guo, X. Cao, N. Wang, Z.L. Wang, All-in-one cellulose based hybrid tribo/piezoelectric nanogenerator, Nano Res. 12 (2019) 1831–1835.
[59] L. Zheng, Z.H. Lin, G. Cheng, W.Z. Wu, X.N. Wen, S.M. Lee, Z.L. Wang, Silicon-based hybrid cell for harvesting solar energy and raindrop electrostatic energy, Nano Energy 9 (2014) 291–300.

Zichao Zhang received his B.S. degree in Chemistry from University of Jinan in 2018. He is currently pursuing a M.S. degree in Guangxi University, and co-trained in Prof. Linlin Li's group in Beijing Institute of Nanoenergy and Nanosystems, Chinese Academy of Sciences. His research interests are focused on self-powered systems and TENG-based sensors.

Qiuyang Yan received her B.S. degree in Wuhan University in 2017 and is now a Ph.D. candidate in SICCAS in Prof. Jing Sun's group. Her research interests are MXenes based flexible electronics.

Zhirong Liu received her B.S. degree from China University of Geosciences in 2016. Currently she is a Ph.D candidate with Prof. Linlin Li at Beijing Institute of Nanoenergy and Nanosystem, Chinese Academy of Science. Her research mainly focuses on bioactive nanomaterials/nanodevices for biomedical applications in drug delivery, stem cell manipulation and tissue regeneration.

Xinyang Zhao received her B.S. degree from Xinyang Normal University of Physics in 2019. She is currently postgraduate at the Shanghai University of Electric Power. She is currently co-trained by Prof. Linlin Li in Beijing Institute of Nanoenergy and Nanosystems, Chinese Academy of Sciences. Her research interests are focused on self-powered nanosystems and TENG-based sensors.

Dr. Zhuo Wang obtained her B.Sc. degree from Liaoning Normal University and Ph.D. degree from the Research Center for Eco-Environmental Sciences, Chinese Academy of Sciences. She was then a postdoctoral fellow at the Department of Chemistry, Tsinghua University. She is currently working at Beijing Institute of Nanoenergy and Nanosystems, CAS. Her research concerns controlled synthesis of nanocomposites and nanomaterials for supercapacitors and batteries.

Prof. Jing Sun: Aiming at the fundamental scientific problems related to the build-up of macroscopic functional systems by nano-units, **Prof. Jing Sun** focused on the investigation of nanomaterials with special functional properties including photocatalysts of high efficiency for indoors & outdoors air-cleaning, metal nanowires and low-dimensional carbon materials such as CNTs, graphene and MXene for flexible strain sensors. She probes the in-depth mechanism of the nano-unit assembly and the functionality enhancement, found novel properties generated from the interfacial coupling effect induced by various components and various scales and realized the high performance of the nanocomposite materials in novel photocatalytic modules and sensors. She published more than 280 scientific papers in journals such as JACS, AM, AFM, etc. The published papers were cited 11000 times and the h-index was 55. She was awarded Shanghai Excellent Academic Leader, Excellent Academic Supervisor of CAS, Awards on the International Cooperation of Young CAS Scientists, etc.

Prof. Zhong Lin Wang received his Ph.D. degree from Arizona State University in physics. He now is the Hightower Chair in Materials Science and Engineering, Regents' Professor at Georgia Tech, the chief scientist and director of the Beijing Institute of Nanoenergy and Nanosystems, Chinese Academy of Sciences. Prof. Wang has made original and innovative contributions to the synthesis, discovery, characterization and understanding of fundamental physical properties of oxide nanobelts and nanowires, as well as applications of nanowires in energy sciences, electronics, optoelectronics and biological science. His discovery and breakthroughs in developing nanogenerators establish the principle and technological road map for harvesting mechanical energy from environmental and biological systems for powering personal electronics. His research on self-powered nanosystems has inspired the worldwide efforts in academia and industry for studying energy for micro-nano-systems, which is now a distinct disciplinary in energy research and future sensor networks. He coined and pioneered the fields of piezotronics and piezophototronics by introducing piezoelectric potential gated charge transport process in fabricating new electronic and optoelectronic devices.

Ranran Wang received her Ph.D. degree (2012) from SICCAS and has been co-cultivated in University of California, Los Angeles for two years (2010–2012). She is now working as a professor in SICCAS. She focuses on the fabrication of low dimensional conductive materials and their application in flexible electronics. She has published 37 papers as the first or the corresponding author and has been selected as the member of Youth Innovation Promotion Association CAS, Shanghai Science and Technology Rising Star Project and Young Elite Scientists Sponsorship Program by CAST. She has filed 21 Chinese patents, 19 of which have been authorized.

Prof. Linlin Li received her M.S. degree in Biochemistry and Molecular Biology from Beijing Normal University in 2005, and Ph.D. degree in Physical Chemistry from Technical Institute of Physics and Chemistry, Chinese Academy of Sciences in 2008. Currently, she is a professor at Beijing Institute of Nanoenergy and Nanosystems, CAS. Her research interests include biomedical application of biomaterials and devices (nanogenerator and piezotronic device) in cancer therapy, biosensing, and tissue regeneration. Details can be found at: https://www.x-mol.com/groups/lilinlin.